MOLECULAR IMAGING AND BIOLOGY

Mol Imaging Biol (2019) 21:852–860
DOI: 10.1007/s11307-019-01326-5

Published Online: 21 February 2019

WMIS World Molecular Imaging Society

Check for updates

RESEARCH ARTICLE

uMUC1-Targeting Magnetic Resonance Imaging of Therapeutic Response in an Orthotropic Mouse Model of Colon Cancer

Hongwei Zhao,[1,2,3] Romani Richardson,[1,4] Nazanin Talebloo,[1,5] Pinku Mukherjee,[6,7] Ping Wang,[1] Anna Moore[1]

[1]*Precision Health Program, Department of Radiology, College of Human Medicine, Michigan State University, 775 Woodlot Dr., Rm. 3.111, East Lansing, MI, 48823, USA*
[2]*Shanxi Medical University, Taiyuan, 030001, Shanxi, China*
[3]*Department of Gynecologic Oncology, Shanxi Provincial Cancer Hospital, Taiyuan, 030013, Shanxi, China*
[4]*Hofstra University, Hempstead, NY, 11549, USA*
[5]*Department of Chemistry, College of Natural Science, Michigan State University, East Lansing, MI, 48824, USA*
[6]*Department of Biological Sciences, University of North Carolina at Charlotte, Charlotte, NC, USA*
[7]*School of Medicine, University of North Carolina at Chapel Hill, Chapel Hill, NC, 27514, USA*

Abstract

Purpose: Noninvasive assessment of chemotherapeutic response in colon cancer would tremendously aid in therapeutic intervention of cancer patients and improve outcomes. The aim of the study was to evaluate the feasibility of a noninvasive assessment of chemotherapeutic response by magnetic resonance imaging utilizing underglycosylated mucin 1 (uMUC1) tumor antigen as a biomarker of therapeutic response in a colon cancer mouse model.

Procedures: The study was performed by applying molecular imaging approach based on targeting uMUC1 with specific dual-modality imaging probe (MN-EPPT). The probe consisted of dextran-coated iron oxide nanoparticles conjugated to the near infrared fluorescent dye Cy5.5 and to a uMUC1-specific peptide (EPPT) and was used for magnetic resonance imaging (MRI) and fluorescence optical imaging. An orthotopic murine model of colon cancer expressing human uMUC1 peptide (MC38 MUC1) was created along with the control model devoid of the antigen (MC38 neo). Animals received chemotherapy with 5-fluorouracil (5-FU) followed by MN-EPPT-enhanced MR and optical imaging.

Results: In vivo imaging of animals with uMUC1 expressing tumors after 5-FU therapy showed that the average deltaT2 was reduced by 7.27 ms ($p = 0.045$) compared with animals in control groups indicating lower accumulation of MN-EPPT caused by uMUC1 downregulation. *In vivo* optical imaging, biodistribution, and fluorescence microscopy confirmed the MRI findings. Interestingly, we found that the group of animals that did not respond to chemotherapy ("progressive disease" per RECIST) showed higher accumulation of MN-EPPT compared to the group of responders ("stable disease") consistent with proliferating tumor cells and increased antigen availability.

Electronic supplementary material The online version of this article (https://doi.org/10.1007/s11307-019-01326-5) contains supplementary material, which is available to authorized users.

Correspondence to: Anna Moore; *e-mail:* moorea57@msu.edu

Conclusions: We believe that in application to over 50 % of human cancers expressing uMUC1, our results could provide insight into overall assessment of therapeutic response based on its expression as defined by non-invasive MN-EPPT-enhanced MRI.

Key Words: Colon cancer, Underglycosylated mucin 1 tumor antigen (uMUC1), *In vivo* molecular imaging, Targeted nanoparticles

Introduction

Malignant cell growth that originates in the large intestine is classified as colon cancer. This type of cancer is especially concerning due to its prevalence, as it ranks the third in terms of incidence and the second in terms of mortality [1]. The correlation between the morbidity and mortality rates of colon cancer reflects on the devastating nature of the disease. The vast majority of colon cancers (95 %) are classified as adenocarcinomas. Current methodology of diagnosing and treating patients is suboptimal: patients that are diagnosed with the same type of cancer and are defined as being at the same stage of cancer progression respond differently to treatment [2]. This variation can be attributed to genetic modifications which cause unique chemotherapeutic responses in each individual. The situation becomes even more complicated when therapeutic response cannot be adequately evaluated due to the lack of appropriate imaging tools. While x-ray computed tomography (CT) remains the most widely used modality for assessing treatment response in colon cancer, it lacks the ability to characterize tumor heterogeneity and tumor evolution over time [3]. In addition, a growing body of evidence suggests that tumor size does not always adequately correlate with clinical outcomes [4], and tracking molecular changes in cancer cells is necessary. Magnetic resonance imaging (MRI) is a versatile technique, which could provide reliable information regarding molecular changes associated with therapy response in combination with target-specific contrast agents.

Underglycosylated mucin 1 (uMUC1) tumor antigen has been identified as one of the prominent biomarkers, which is overexpressed in various adenocarcinomas including colon cancer [5]. Our previous studies have demonstrated the utility of uMUC1 as a biomarker for monitoring breast and pancreatic cancer progression and response to therapy using non-invasive magnetic resonance imaging [6–8]. To monitor the expression of uMUC1 in tumors using MRI, we utilized an imaging probe consisting of iron oxide nanoparticles conjugated to an uMUC1-specific peptide (MN-EPPT, [6]). Studies have shown that the level of MN-EEPT accumulation in tumors directly correlate with uMUC1 expression. In this study, we investigated whether the level of uMUC1 expression in colon cancer would follow the rate of MN-EPPT accumulation and whether chemotherapy would have an impact on monitoring therapeutic response by MRI. Using orthotopic murine model of colon cancer expressing human mucin 1 tumor antigen we demonstrated that chemotherapy with 5-Fluorouracil caused downregulation of uMUC leading to the reduced accumulation of the imaging probe. This observation could have implications on prediction of treatment outcome as the changes in uMUC1 expression preceded significant changes in tumor size.

Materials and Methods

MN-EPPT Synthesis

Iron oxide magnetic nanoparticles (MN) conjugated to the EPPT peptide (C-AHA-Y-C(ACM)-A-R-E-P-P-T-R-T-F-A-Y-W-G-K) were synthesized as described previously [8]. MN-EPPT was synthesized to contain near infrared optical dye for correlative near infrared optical imaging (NIRF) and fluorescence microscopy [8]. The number of EPPT peptides on MN was quantified by BCA protein assay and the number of Cy5.5 dye molecules on MN was quantified spectrophotometrically. The loading ratio of EPPT and Cy5.5 per MN was 8.7 and 2.3 respectively. We also synthesized control nanoparticles contained scrambled EPPT sequence (MN-SCR). These nanoparticles were identical to MN-EPPT except for the peptide sequences which were the EPPT scrambled sequence (C-AHA-A-E-G-R-P-T-F-P-T-R-A-Y-W-K).

In vitro Cell Binding Assay

MC38 MUC1 (expressing human MUC1) and MC38 neo (mock-transduced negative control) cell lines derived from C57BL6 murine colon adenocarcinoma cells were provided by Dr. Pinku Mukherjee (University of North Carolina, [9]). MC38 cells were originally a gift from Dr. Jeffrey Schlom (Bethesda, MD). To assess relative accumulation of the imaging probes in these cells, two cell lines were seeded into 96-well plates and incubated with MN-EPPT and MN-SCR (0, 12.5, 25, 50, and 100 μg/ml Fe) respectively at 37 °C for 1 h. After incubation, Cy5.5 fluorescence levels were measured using an IVIS spectrum imaging system (PerkinElmer, Hopkinton, MA), and normalized to total cell protein determined by bicinchoninic acid protein assay (BCA assay, Pierce, Thermo Fisher Scientific, Inc., Rockford, IL). To examine if 5-fluorouracil (5-FU, Sigma) could downregulate uMUC1 expression, MC38 MUC1 cells were incubated with 0.2 μmol/l 5-FU at 37 °C for 24 h. Cells not treated with 5-FU served as a negative control. To assess if relative accumulation of MN-EPPT was proportional to uMUC1 expression following treatment with 5-FU, the cells

were incubated with MN-EPPT at 37 °C for 1 h. Following incubation, the cells were analyzed for uMUC1 expression by immunocytochemistry. Cells were stained with hamster monoclonal anti-mucin 1 antibody (MH1, 1:100 dilution; ThermoFisher, Carlsbad, CA), followed by incubation with corresponding FITC-labeled IgG secondary antibody (1:200 dilution; Abcam, Cambridge, MA), counterstained with DAPI (Vectashield; Vector Laboratories, Inc., Burlingame, CA) for cell nucleus staining.

Fluorescent images were examined using a Nikon Eclipse 50i fluorescence microscope (Nikon, Melville, NY), equipped with the necessary filter sets and analyzed using SPOT 4.0 Advance version software (Diagnostic Instruments, Sterling Heights, MI).

Orthotopic Colon Cancer Animal Model

All applicable institutional and/or national guidelines for the care and use of animals were followed. Orthotopic colon cancer tumor model was established in isoflurane-anesthetized 8-week-old female C57BL/6 mice (Jackson Laboratories, Bar Harbor, ME) first by subcutaneous injection of 1×10^6 of either MC38 MUC1 or MC38 neo cells into the right flank of a mouse. When subcutaneous tumor reached 0.5 cm in diameter, it was excised and cut into nodules of approximately 1 mm in diameter. To establish an orthotopic tumor model of colon cancer, the tumor nodules were surgically implanted in the cecum of 8-week-old female C57BL/6 mice through a median incision made in the lower abdomen. Briefly, the peritoneum was separated from the abdominal wall and opened. The cecum was exposed and a tumor nodule was embedded into cecum on the mesentery side with interrupted sutures using 5.0 Vicryl (Ethicon, Somerville, NJ). Both peritoneum and abdominal wall were then closed. Monitoring of the tumor growth was performed by MRI using a 9.4-T Bruker horizontal scanner equipped with a Rat Array MRI CryoProbes coil. Chemotherapy with 5-FU was started when the tumor size reached at least 0.5 cm in diameter (approximately 4 weeks after implantation). The difference in MN-EPPT uptake before and post chemotherapy in MC38 MUC1 and MC neo colon tumors was evaluated by MRI after intravenous injection of MN-EPPT or MN-SCR. The course of the studies is presented in Table 1. The description of experimental and control groups is presented in detail in Table 2.

Table 1. Timeline for chemotherapy and *in vivo* imaging experiments

Days	0	7	14	21	28	30
Chemotherapy		X	X	X	X	
MRI	X			X		X
Optical imaging	X			X		X

Treatment and Response Evaluation Criteria

To establish a clinically relevant treatment model, we chose 5-fluorouracil as a chemotherapy drug. 5-FU is one of pyrimidine analogues, which exerts its antitumor effects by inhibiting DNA/RNA synthesis, and is approved as a therapeutic agent against colon cancer in clinic. One round of the treatment protocol involved intraperitoneal injections of 30 mg/kg of 5-FU in saline solution once daily for 5 consecutive days with a therapy break on the following 2 days. The total of four rounds of therapy was performed (Table 1). Saline solution-injected animals served as nontreated controls. To evaluate tumor response to chemotherapy, *in vivo* imaging was performed 1 day before and 1 day following the completion of the two rounds of chemotherapy (Table 1). Treatment outcome, as reflected by the change in tumor longest diameter, was compared before and after treatment every two rounds of chemotherapy. According to response evaluation criteria in solid tumors (RECIST), complete response (CR): disappearance of the target lesion; partial response (PR): ≥ 30 % decrease in the longest diameter of target lesion compared with baseline; progressive disease (PD): ≥ 20 % increase in the longest diameter of target lesion compared with baseline recorded or the appearance of one or more new lesions; stable disease (SD): neither PR or PD. Generally, CR, PR, and SD would be considered as an effective result of chemotherapy and PD would be considered ineffective.

Magnetic Resonance Imaging

For every two rounds chemotherapy, *in vivo* MRI was performed on MC38 MUC1 and MC neo-bearing animals before and 24 h after intravenous injection of MN-EPPT or MN-SCR (15 mg Fe/kg) (Table 1), using a 9.4 T Bruker horizontal bore scanner equipped with a Rat Array MRI CryoProbes coil (Bruker, Billerica, MA). Iron oxide-based contrast agents cause the tissue signal loss on T2-weighted sequences due to the susceptibility effects of the iron oxide core, and therefore can be used for tumor delineation. The size of the tumors was evaluated using the longest diameter. T2 relaxation times of the tumors were evaluated by free-hand segmenting of the region of interest (ROI) on MRI. ROIs were selected to include the entire tumor visible on a particular slice. Relative MN-EPPT/MN-SCR accumulation in the tumors was calculated according to the following formula: $\delta T2(\text{delta-T2, in milliseconds}) = T2$ before injection-T2 after injection. T2 map was analyzed voxel-by-voxel by fitting the T2 measurements to a standard exponential decay curve, defined by the following formula: $y = A \exp.(-t/T2)$ using MATLAB software R2011b (The MathWorks, Inc., Natick, MA). Average T2 times in manually selected ROIs surrounding the targeted tumors were calculated using ImageJ software 1.50c (NIH, Bethesda, MD). Image analysis was performed by two independent investigators blinded to sample identities.

Table 2. Experimental group and control groups

Groups	Sample#	Xenograft model	Chemotherapy regimen	MRI probe	Imaging
Experimental group	7	MC 38 muc1	5-FU for 4 rounds	MN-EPPT	3 rounds
Control group 1	3	MC 38 muc1	Saline control	MN-EPPT	3 rounds
Control group 2	3	MC 38 muc1	Saline control	MN-SCR	3 rounds
Control group 3	3	MC 38 neo	None	MN-EPPT	1 round
Control group 4	3	MC 38 neo	None	MN-SCR	1 round

In vivo and Ex vivo Epifluorescence Optical Imaging

In vivo epifluorescence optical imaging was performed to corroborate the accumulation of the imaging probes in the tumors utilizing the signal from Cy5.5 dye conjugated to the nanoparticles. The timeline of the optical imaging was same as that of MRI. It was performed immediately after each MRI session using an IVIS spectrum animal imaging system (PerkinElmer, Hopkinton, MA). To evaluate the imaging results, an ROI was drawn around each tumor and image analysis was conducted using LivingImage 4.2 software (PerkinElmer, Hopkinton, MA). Average fluorescence signal efficiency, defined as fluorescence emission normalized to the incident excitation intensity (radiance of the subject/illumination intensity), was used for quantification. After the last imaging session, mice were sacrificed; tumors and tissues were excised and imaged *ex vivo* for the biodistribution using the IVIS spectrum system. The organs included liver, spleen, kidney, lung, heart, intestine, and muscle. Image analysis was performed using the LivingImage 4.2 software (PerkinElmer, Hopkinton, MA).

Histology and Immunostaining

Correlative immunohistochemistry (IHC) was performed to evaluate the expression of uMUC1 and the accumulation of MN-EPPT/MN-SCR in tumors. Immunohistochemistry was performed on frozen sections derived from tumors in cecum by staining for uMUC1 and colocalizing it with Cy5.5 signal derived from the MN-EPPT or MN-SCR probe. Tumors were embedded in Tissue-Tek OCT compound and cut into 7 μm frozen sections. The dilutions of anti-mucin 1 antibody and FITC-labeled IgG secondary antibody were same as those used for immunocytochemistry (ICC) mentioned above. The staining results were analyzed using a Nikon Eclipse 50i fluorescence microscope equipped with an appropriate filter set (Chroma Technology Corporation). Images were acquired using a charge-coupled device camera with near-IR sensitivity (SPOT 7.4 Slider RTKE, Diagnostic Instruments). Fluorescence of FITC, DAPI, and Cy5.5 was collected in appropriate channels. Investigators blinded to the animal treatment groups analyzed all tissue sections using SPOT 4.0 advance version software (Diagnostic Instruments, Sterling Heights, MI).

Statistical Analysis

Data were presented as mean±SD. Statistical comparisons between two groups were evaluated by the Student *t* test and corrected by one-way ANOVA for multiple comparisons using GraphPad Prism 5 (GraphPad Software, Inc., La Jolla, CA, USA). A value of $P < 0.05$ was considered statistically significant.

Results

MN-EPPT Specific Accumulation in MC38 MUC1 Cells and Tumors

To evaluate the accumulation of MN-EPPT and MN-SCR in MC38 MUC1 cell, the cells were incubated with the probes at 37 °C for 1 h. As seen in Fig. 1a and b, MC38 MUC1cells demonstrated significantly higher, concentration-dependent accumulation of MN-EPPT compared to MN-SCR. There was no significant difference in accumulation of neither probes in MC38 neo cells.

Fluorescence microscopy was used to evaluate changes in uMUC1 expression following 5-FU treatment of MC38 MUC1cell. As seen in Fig. 1c, uMUC1 expression decreased following treatment with 5-FU. This followed the accumulation of MN-EPPT, which was decreased in MC38 MUC1 cell following treatment with 5-FU as assessed by Cy5.5 fluorescence.

The above results were mirrored by the *in vivo* biodistribution studies that demonstrated preferential accumulation of MN-EPPT in the tumor lesions compared to other surrounding organs (Fig. 2a and b). Importantly, these findings supported our *in vitro* data (Fig. 1c) and showed the tendency of uMUC1 expression to decrease in response to cancer treatment as evident from the difference in signal intensity that signifies MN-EPPT accumulation between the experimental and control groups (Fig. 2b).

MN-EPPT-Enhanced Molecular Imaging Permits Monitoring of Chemotherapy Response

The tumor size in 5-FU-treated animals were assigned according to RECIST as described in "Materials and Methods". Specifically, after four rounds of chemotherapy, tumors of five mice were categorized as SD and tumors of

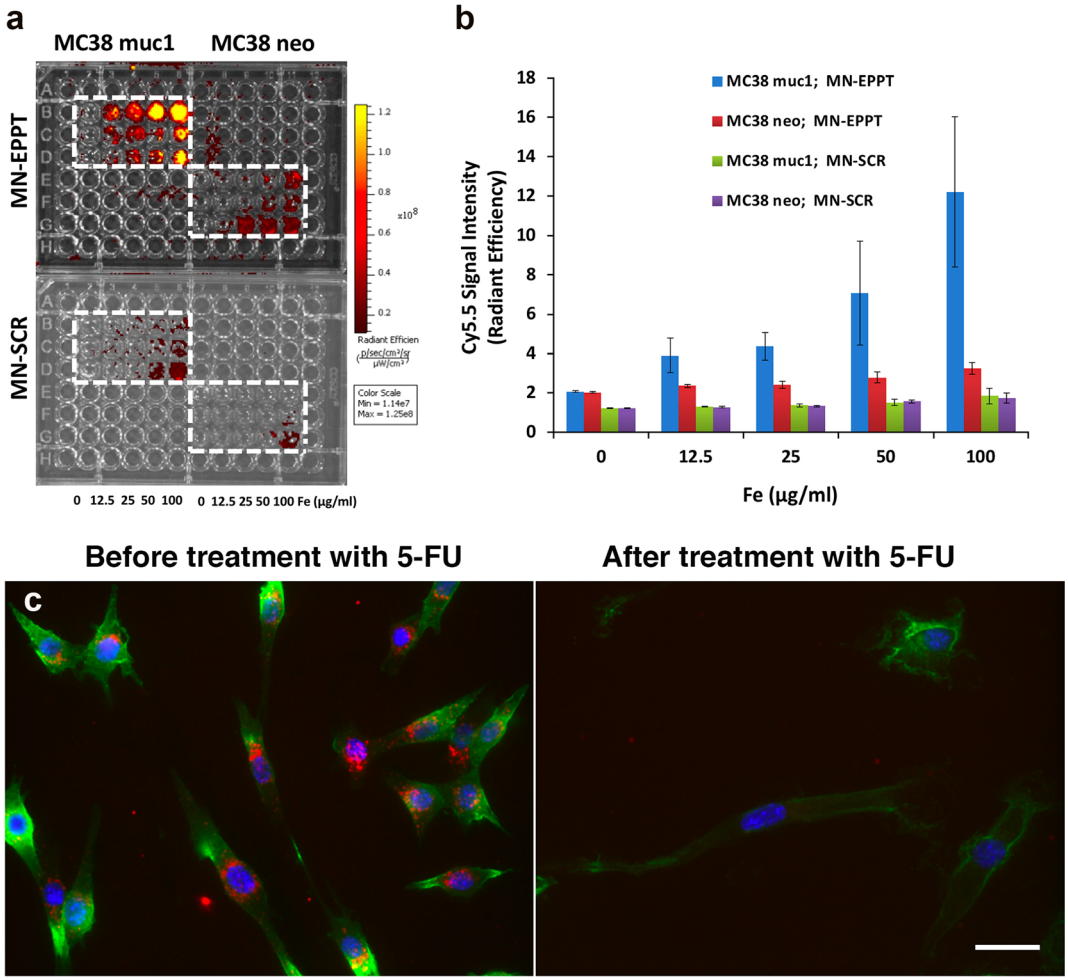

Fig. 1. **a***In vitro* testing of MN-EPPT and MN-SCR accumulation in MC38 MUC1 and MC38 neo cell lines. **b** Cell binding assays showed concentration-dependent preferential uptake of experimental MN-EPPT probe by MC38 MUC1cells compared to control probes. There was no difference in uptake between the experimental and control probes by the control MC38 neo cell line. **c** Fluorescence microscopy of MC38 MUC1cells before (left) and after (right) 5-FU treatment. Note changes in uMUC1 expression and reduced MN-EPPT accumulation in treated cells (green, uMUC1; red, Cy5.5 dye conjugated to nanoparticles; blue, DAPI, cell nucleus; magnification bar = 15 µm).

two mice were PD. In all nontreated animals, the diameter of lesions doubled in 4 weeks. As for MRI results, after four rounds of chemotherapy, tumor delta-T2 values in the control group 1 were significantly higher than in the experimental group as showed in Fig. 3a and b (23.50 ± 2.98 ms *vs.* 16.23 ± 4.84 ms). We also observed the smaller delta-T2 in the SD mice than in the PD mice (Fig. 3c). Optical imaging confirmed these results and showed that the overall fluorescence intensity associated with the lesions in the PD mice remained higher than in the SD mice (Suppl. Fig. 1, see Electronic Supplementary Material (ESM)). In addition, to confirm the specificity of uMUC1 targeting probe *in vivo*, non-treated animals bearing MC38 neo xenografts devoid of uMUC1 were injected with MN-EPPT or MN-SCR probe (control groups 3 and 4) followed by MRI. The results showed that there was no difference in delta-T2 values between these two groups (Fig. 3d). Similarly, optical imaging showed no statistical differences in fluorescence signal intensity between these groups (Suppl. Fig. 2, see ESM). These findings demonstrate that uMUC1 expression has the tendency to decrease in response to cancer treatment.

Ex vivo Analysis of MN-EPPT Accumulation and uMUC1 Expression

To further confirm *in vivo* imaging results, the cecum tumor sections derived from 5-FU treated (experimental group) and nontreated (control group) mice were stained for uMUC1 expression and accumulation of MN-EPPT. The results showed uMUC1 expression not only in the cytomembrane but also in the cytoplasm of tumor cells, which distributed throughout the disorganized glandular epithelium of cecum

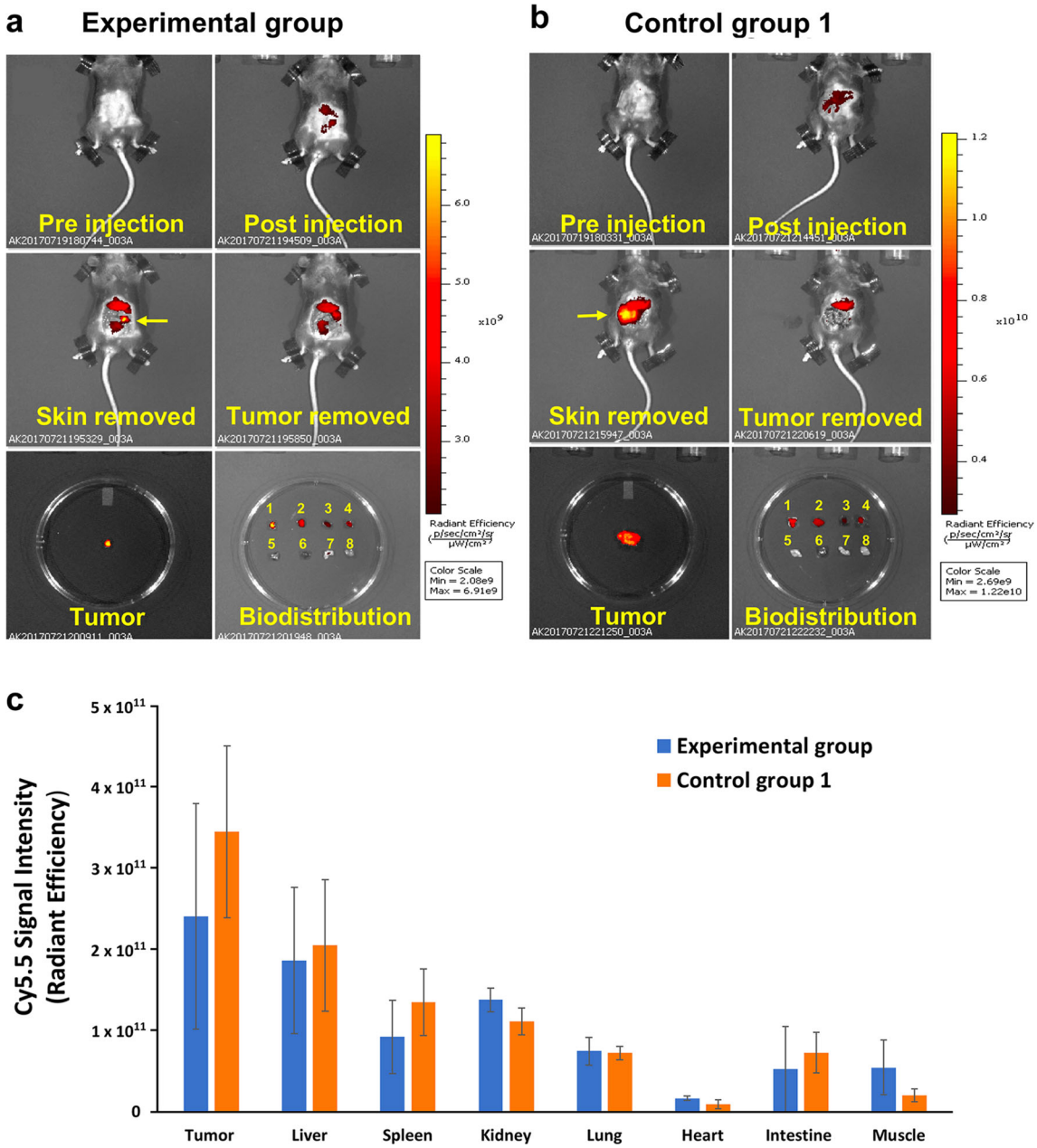

Fig. 2. *In vivo* optical imaging after 4 rounds of chemotherapy with 5-FU. There were visible differences in fluorescence intensity of Cy5.5 in tumors between **a** the experimental and **b** non-treated control animals. Note the disappearance of the optical signal from the tumor upon tissue removal signifying the specificity of MN-EPPT. Tissue labels in petri dish: 1, tumor; 2, liver; 3, spleen; 4, kidney; 5, lung; 6, heart; 7, intestine; 8, muscle. **c** Biodistribution showed lower uptake of MN-EPPT in experimental treated animals consistent with uMUC1 downregulation. Note that there was no statistical differences in the uptake by major organs between experimental and non-treated control group.

tumor lesions (Fig. 4). Protein expression of uMUC1 in the SD mice was lower than in the PD mice or the nontreated mice. Accumulation of MN-EPPT, which was judged by Cy5.5 fluorescence, was lower than in the SD mice compared to the PD mice or nontreated mice (Fig. 4). We concluded that the accumulation of the MN-EPPT in these lesions reflects uMUC1 expression, which clearly decreases in response to chemotherapy.

Discussion

MUC1 is a glycoprotein that prevents pathogens from reaching the cell surface [10]. Overexpression and underglycosylation of MUC1 is often associated with colon, breast, ovarian, lung, and pancreatic cancers [11]. Our previous *in vivo* animal studies demonstrated that the changes in uMUC1 expression in breast and pancreatic cancers treated with chemotherapy could be

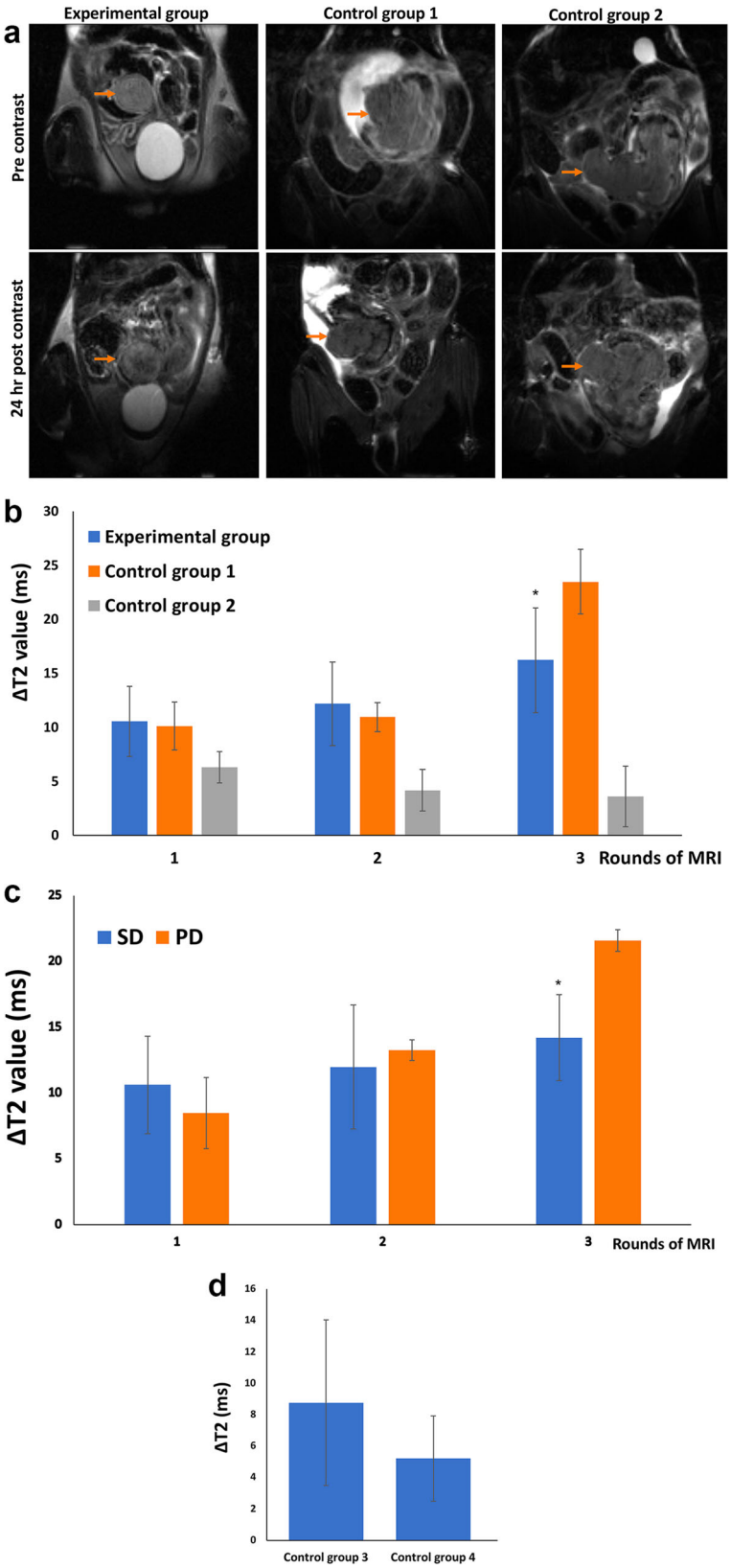

Fig. 3. MN-EPPT-enhanced MRI. **a** Pre- and post-contrast images of experimental and control animals showing accumulation of MN-EPPT in tumors (arrows). **b** The deltaT2 values of the tumors in animals from experimental group were significantly decreased (*$P < 0.05$) compared to control group 1 that did not receive chemotherapy. **c** Quantitative analysis of deltaT2 value changes shows significant differences in T2 relaxation times between tumors from SD or PD animals in experimental group (*$P < 0.05$). **d** There were no statistically significant differences in deltaT2 values between control groups 3 and 4.

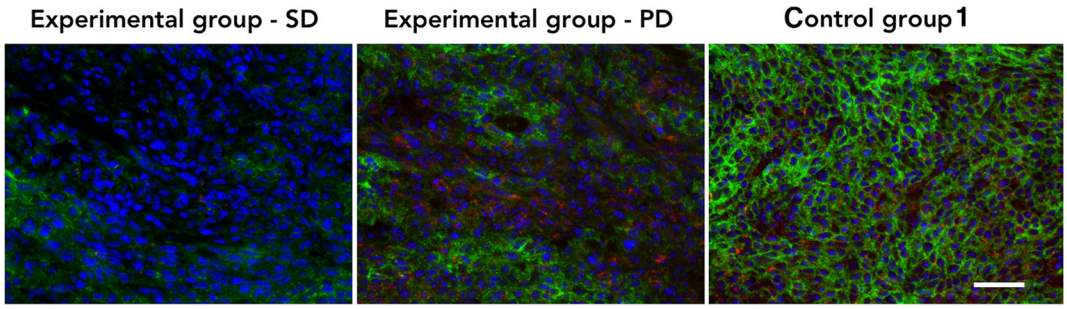

Fig. 4. Fluorescence microscopy demonstrates changes in uMUC1 expression and MN-EPPT accumulation in tumors from SD or PD animals from experiments group (green, uMUC1; red, Cy5.5 dye conjugated to nanoparticles; blue, DAPI, cell nucleus; magnification bar = 50 μm).

detected using MN-EPPT-enhanced MRI [7, 8]. Therefore, in this current study, we hypothesized that uMUC1 could be regarded as a prognostic biomarker of therapeutic response for colon cancer thus providing the ability to monitor response to chemotherapy on a molecular level and permitting early and more adequate therapeutic intervention. To monitor the changes in uMUC1 expression in response to chemotherapy, we utilized *in vivo* MRI with uMUC1-specific MN-EPPT probe. Accumulation of this probe is detectible by MRI due to the strong magnetization force of iron, which disrupts the surrounding protons of water, reporting a low-intensity signal on the MR images [12]. Our results support previous findings showing the reduction of uMUC1 expression in breast cancer and pancreatic cancer [7, 8], as detected by the changes in average deltaT2 value after chemotherapy. The results from the current study support our earlier findings that changes in uMUC1 expression precede changes in other anatomical and/or physiological indications of therapeutic progress. In fact, we established a new finding that tumors that were not responsive to the treatment and that were classified as "progressive disease," accumulated significantly higher amount of the MN-EPPT probe due to continuous cell proliferation and increased availability of uMUC1 antigen. On the other hand, MN-EPPT accumulation was reduced in the tumors that responded to therapy (classified as "stable disease"), pointing to reduced uMUC1 expression. These results demonstrate that MRI permits for stratification of tumor-bearing animals based on their response to 5-FU therapy. Also, these findings might reflect a clinical situation when patients respond to the same chemotherapy differently [13, 14].

As in our previous studies [7, 8], we believe that uMUC1 downregulation is not a result of a specific action of 5-FU but rather the overall response of the dying tumor cell to a pro-apoptotic stimuli imposed by the drug. Investigation of the mechanisms behind 5-FU action contributing to uMUC1 downregulation is a subject of a separate study that is currently under way in our laboratory.

In this study, the contrast agent was not used for imaging tumor volume but rather for imaging the relative expression of the uMUC1 tumor antigen, as a biomarker of therapeutic response. Tumor volume is a late and relatively ineffective parameter because changes in tumor volume may not be visible in a responder population for some time after the beginning of treatment. Therefore, it would also be a late and ineffective parameter in identifying non-responders. In fact, in our study, changes in tumor size were not obvious until the end of the treatment schedule. Generally, our results point to the necessity to evaluate "target-specific" imaging for tumor detection more carefully when it is used in conjunction with therapy as the specific tumor biomarker could be downregulated in response to said therapy thus skewing imaging results. In application to over 50 % of human cancers expressing uMUC1 [15], our results could provide insight into overall assessment of therapeutic response based on its expression as defined by non-invasive MN-EPPT-enhanced MRI.

Acknowledgments. The authors would like to thank Dr. Byunghee Yoo (Massachusetts General Hospital) for his help in synthesizing magnetic imaging probes, Dr. Chris Farrar (Massachusetts General Hospital) for help with MR imaging analysis and Dr. Zdravka Medarova (Massachusetts General Hospital) for helpful discussion.

Funding Information. This work was supported in part by the grant R01CA135650, Charlotte Research Institute and the Vivarium staff at the University of North Carolina.

Compliance with Ethical Standards

Conflict of Interest

The authors declare that they have no conflict of interest.

References

1. http://www.iarc.fr/en/media-centre/pr/2018/pdfs/pr263_E.pdf Press Release No 263. (accessed September 12)
2. Yang R, Niepel M, Mitchison T, Sorger P (2010) Dissecting variability in responses to cancer chemotherapy through systems pharmacology. Clin Pharmacol Ther 88:34–38
3. McKeown E, Nelson DW, Johnson EK, Maykel JA, Stojadinovic A, Nissan A, Avital I, Brücher BLDM, Steele SR (2014) Current approaches and challenges for monitoring treatment response in colon and rectal cancer. J Cancer 5:31–43

4. Custem EV, Verheul HM, Flamen P et al (2016) Imaging in colorectal cancer: progress and challenges for the clinicians. Cancers (Basel) 8:E81
5. Hollingsworth MA, Swanson BJ (2004) Mucins in cancer: protection and control of the cell surface. Nat Rev Cancer 4:45–60
6. Moore A, Medarova Z, Potthast A, Dai G (2004) *In vivo* targeting of underglycosylated MUC-1 tumor antigen using a multimodal imaging probe. Cancer Res 64:1821–1827
7. Ghosh SK, Uchida M, Yoo B, Ross AW, Gendler SJ, Gong J, Moore A, Medarova Z (2013) Targeted imaging of breast tumor progression and therapeutic response in a human uMUC-1 expressing transgenic mouse model. Int J Cancer 132:1860–1867
8. Wang P, Yoo B, Sherman S, Mukherjee P, Ross A, Pantazopoulos P, Petkova V, Farrar C, Medarova Z, Moore A (2016) Predictive imaging of chemotherapeutic response in a transgenic mouse model of pancreatic cancer. Int J Cancer 139:712–718
9. Mukherjee P, Pathangey L, Bradley J et al (2006) MUC1-specific immune therapy generates a strong anti-tumor response in a MUC1-tolerant colon cancer model. Vaccine 25:1607–1618
10. Moncada DM, Kammanadiminti SJ, Chadee K (2003) Mucin and toll-like receptors in host defense against intestinal parasites. Trends Parasitol 19:305–311
11. Gendler SJ (2001) MUC1, the renaissance molecule. J Mammary Gland Biol Neoplasia 6:339–353
12. Nelson CA (2008) Incidental findings in magnetic resonance imaging (MRI) brain research. J Law Med Ethics 36:315–319, 213
13. Linnekamp JF, Wang X, Medema JP, Vermeulen L (2015) Colorectal cancer heterogeneity and targeted therapy: a case for molecular disease subtypes. Cancer Res 75:245–249
14. Sagaert X, Vanstapel A, Verbeek S (2018) Tumor heterogeneity in colorectal cancer: what do we know so far? Pathobiology 85:72–84
15. Strous GJ, Dekker J (1992) Mucin-type glycoproteins. Crit Rev Biochem Mol Biol 27:57–92